

Selenium-Based Self-Assembled Monolayers: The Nature of
Adsorbate–Surface Interactions

Ezequiel de la Llave and Damián A. Scherlis*

*Departamento de Química Inorgánica, Analítica y Química Física/INQUIMAE, Facultad de Ciencias Exactas y Naturales, Universidad de Buenos Aires, Ciudad Universitaria, Pab. II, Buenos Aires C1428EHA, Argentina**Received April 13, 2009. Revised Manuscript Received October 31, 2009*

In recent years, self-assembled monolayers (SAMs) of selenols have been characterized using electrochemistry, scanning tunneling microscopy (STM), X-ray photoelectron spectroscopy (XPS), thermal desorption spectroscopy, and other experimental approaches. Interest in the relative stability and conductance of the Se–Au interface as compared to S–Au prompted different investigations which have led to contradictory results. From the theoretical side, on the other hand, the study of selenol-based SAMs has concentrated on the investigation of the electron transport across the Se–Au contact, whereas the structural and the thermodynamic features of the monolayer were essentially neglected. In this Article, we examine the binding of selenols to the Au(111) surface using density functional theory with plane wave basis sets and periodic boundary conditions. Our calculations provide insights on the geometry of the headgroup, the stability of the monolayer, and the electronic properties of the bond. In particular, we propose that the presence of a conjugated backbone might be a major factor determining the relative conductance at the monolayer, by differentially enhancing the intramolecular electron transport in selenols with respect to thiols. This surmise, if confirmed, would explain the conflictive data coming from the available experiments.

I. Introduction

In the last two decades, we have attended to a rapid evolution of the knowledge and understanding concerning the binding of molecules to metal and semiconducting surfaces. This interest arises from the broad range of possibilities that the covalent attachment of molecules to surfaces offers in such diverse areas as advanced coatings, sensors, hybrid materials, or molecular electronics. Foremost examples of this chemistry are the self-assembled monolayers (SAMs) of thiols, which provide a convenient, flexible, and simple system to tailor the interfacial properties of metals, metal oxides, and semiconductors.^{1,2} More recently, synthetic routes have been developed for the binding of molecules to different metallic substrates using carbon instead of sulfur as the link atom. Works emanating from both the experimental and theoretical sides have been reported, discussing the nature of carbon-based SAMs bound to gold^{3–8} and to other materials.^{9–12}

On the other hand, selenium has been regarded as a viable alternative to sulfur for building SAMs ever since the first

evidence of selenol monolayers was published by Samant et al.¹³ Soon after this paper, Dishner and co-workers used scanning tunneling microscopy (STM) to claim the deposition of ordered monolayers of diphenyl diselenide and benzeneselenol on Au(111).¹⁴ Many other experiments followed that confirmed the formation of SAMs bound to a metal surface via a selenium atom. A number of studies combining electrochemical and spectroscopical techniques assessed the stability and characterized the formation of ordered monolayers from different selenides and selenols on the Au surface,^{15–20} on Au nanoparticles,^{21–23} and also on the Ag(111) surface.^{24,25}

On the basis of theoretical calculations, different authors have pointed that the replacement of sulfur by selenium in a conjugated molecular wire produces an increase in the conductance across the device. Whereas Ratner et al.²⁶ estimated a 25-fold increase in the conductance, later results by Di Ventra and Lang predicted a 3-fold increase for the same system.²⁷ Using data from ultraviolet

(1) Love, J. C.; Estroff, L. A.; Kriebel, J. K.; Nuzzo, R. G.; Whitesides, G. M. *Chem. Rev.* **2005**, *105*, 1103.

(2) Vericat, C.; Vela, M. E.; Benitez, G. A.; Martin Gago, J. A.; Torrelles, X.; Salvarezza, R. C. *J. Phys.: Condens. Matter* **2006**, *18*, 867.

(3) Seshadri, K.; Atre, S. V.; Tao, Y.-T.; Lee, M.-T.; Allara, D. L. *J. Am. Chem. Soc.* **1997**, *119*, 4698.

(4) Bernard, M.-C.; Chausse, A.; Cabet-Deliry, E.; Chehimi, M. M.; Pinson, J.; Podvorica, F.; Vautrin-UI, C. *Chem. Mater.* **2003**, *15*, 3450.

(5) Laforgue, A.; Addou, T.; Belanger, D. *Langmuir* **2005**, *21*, 6855.

(6) de la Llave, E.; Ricci, A.; Calvo, E. J.; Scherlis, D. A. *J. Phys. Chem. C* **2008**, *112*, 17611.

(7) Jiang, D. E.; Sumpter, B. G.; Dai, S. *J. Am. Chem. Soc.* **2006**, *128*, 6030.

(8) Ricci, A.; Bonazzola, C.; Calvo, E. *J. Phys. Chem. Chem. Phys.* **2006**, *8*, 4297.

(9) Allongue, P.; Delamar, M.; Desbat, B.; Fagebaume, O.; Hitmi, R.; Pinson, J.; Saveant, J.-M. *J. Am. Chem. Soc.* **1997**, *119*, 201.

(10) Adenier, A.; Bernard, M.-C.; Chehimi, M. M.; Cabet-Deliry, E.; Desbat, B.; Fagebaume, O.; Pinson, J.; Podvorica, F. *J. Am. Chem. Soc.* **2001**, *123*, 4541.

(11) Strano, M. S.; Dyke, C. A.; Urey, M. L.; Barone, P. W.; Allen, M. J.; Shan, H.; Kittrell, C.; Hauge, R. H.; Tour, J. M.; Smalley, R. E. *Science* **2003**, *301*, 1519.

(12) Stewart, M. P.; Maya, F.; Kosynkin, D. V.; Dirk, S. M.; Stapleton, J. J.; McGuinness, C. L.; Allara, D. L.; Tour, J. M. *J. Am. Chem. Soc.* **2004**, *126*, 370.

(13) Samant, M. G.; Brown, C. A.; Gordon, J. G., II. *Langmuir* **1992**, *8*, 1615.

(14) Dishner, M. H.; Hemminger, J. C.; Feher, F. J. *Langmuir* **1997**, *13*, 4788.

(15) Huang, F. K.; Horton, R. C., Jr.; Myles, D. C.; Garrell, R. L. *Langmuir* **1998**, *14*, 4802.

(16) Nakamura, T.; Kimura, R.; Matsui, F.; Kondoh, H.; Ohta, T.; Sakai, H.; Abe, M.; Matsumoto, M. *Langmuir* **2000**, *16*, 4213.

(17) Nakano, K.; Sato, T.; Tazaki, M.; Takagi, M. *Langmuir* **2000**, *16*, 2225.

(18) Monnell, J. D.; Stapleton, J. J.; Jackiw, J. J.; Dunbar, T.; Reinert, W. A.; Dirk, S. M.; Tour, J. M.; Allara, D. L.; Weiss, P. S. *J. Phys. Chem. B* **2004**, *108*, 9834.

(19) Sato, Y.; Mizutani, F. *Phys. Chem. Chem. Phys.* **2004**, *6*, 1328.

(20) Käfer, D.; Bashir, A.; Witte, G. *J. Phys. Chem. C* **2007**, *111*, 10546.

(21) Brust, M.; Stühr-Hansen, N.; Nørgaard, K.; Christensen, J. B.; Nielsen, L. K.; Bjørnholm, T. *Nano Lett.* **2001**, *1*, 189.

(22) Yee, C. K.; Ulman, A.; Ruiz, J. D.; Parikh, A.; White, H.; Rafailovich, M. *Langmuir* **2003**, *19*, 9450.

(23) Zelakiewicz, B. S.; Yonezawa, T.; Tong, Y. *J. Am. Chem. Soc.* **2004**, *126*, 8112.

(24) Shaporenko, A.; Müller, J.; Weidner, T.; Terfort, A.; Zharnikov, M. *J. Am. Chem. Soc.* **2007**, *129*, 2232.

(25) Shaporenko, A.; Ulman, A.; Terfort, A.; Zharnikov, M. *J. Phys. Chem. B* **2005**, *109*, 3898.

(26) Yaliraki, S. N.; Kemp, M.; Ratner, M. A. *J. Am. Chem. Soc.* **1999**, *121*, 3428.

(27) Di Ventra, M.; Lang, N. D. *Phys. Rev. B* **2001**, *65*, 45402.

photoemission spectroscopy (UPS) and within the framework of the scattering theory of transport, Patrone and co-workers concluded that Se-termination provides a better electronic coupling to Au than the S headgroup.²⁸ A few experimental studies have been conducted on molecule–Au(111) interfaces which support these results, including STM measurements on thiol and selenol terminated terthiophenes,^{29,30} and combined X-ray photoelectron spectroscopy (XPS)–UPS investigations on benzenethiol and benzeneselenol.³¹ Findings from these works, however, are in apparent contradiction with later STM experiments establishing the opposite trend, that is, that alkanethiolates have a lower barrier to tunneling.³² New calculations and experiments would be desirable to clarify the source of this disagreement. In any case, and beyond all possible discrepancies between calculations and measurements, or between different experiments, the development of selenol-based SAMs appears to be particularly promising for applications in molecular electronics where the contact resistance of the anchoring group is of crucial importance for the electronic transport.³³

Strikingly, most of the theoretical work on the selenolate–gold interface has been focused on the transport properties of the junction, while the other structural and energetic aspects of the interaction have been barely investigated from a theoretical point of view. Equilibrium geometries, charge distributions, and HOMO–LUMO energy gaps were obtained for simplified models consisting of alkaneselenolates linked to clusters of one, two, and three metal atoms.³⁴ To the best of our knowledge, the only work to study from first principles the interaction of selenium with a periodic slab has been limited to the adsorption of the Se atom at different coverages, and aimed to establish possible differences between S- and Se-based metal–molecule interfaces.³⁵ In view of this, we set out to accomplish a more realistic description of the interaction between selenols and gold from a molecular perspective. In this work, we perform periodic density functional calculations on the adsorption of two representative types of selenols (benzeneselenol and methylselenol) on the Au(111) surface. Our motivation is to provide an energetic, structural, and electronic characterization of the bond which is missing in the literature and that can be useful to experimentalists and theoreticians working in this field.

II. Methodology

The Au(111) surface was modeled as an infinite bidimensional stack of slabs, with each slab consisting of four layers of Au atoms truncated at the (111) geometry and separated from the next one by a vacuum region of about 12 Å, enough to render the mutual interactions negligible. Simulations were performed on supercells containing 12 metallic atoms per layer, with dimensions $x = 10.03$ Å, $y = 8.68$ Å, $z = 20.06$ Å (where z is the direction perpendicular to the slab) conforming to the optimized lattice constant of 4.18 Å obtained for the fcc unit cell, which compares well with the experimental value of 4.08 Å. All calculations have been performed using density functional theory (DFT),^{36,37} as

(28) Patrone, L.; Palacin, S.; Charlier, J.; Armand, F.; Bourgojn, J. P.; Tang, H.; Gauthier, S. *Phys. Rev. Lett.* **2003**, *91*, 96802.

(29) Patrone, L.; Palacin, S.; Bourgojn, J. P.; Lagoute, J.; Zambelli, T.; Gauthier, S. *Chem. Phys.* **2002**, *281*, 325.

(30) Patrone, L.; Palacin, S.; Bourgojn, J. P. *Appl. Surf. Sci.* **2003**, *212–213*, 446.

(31) Yokota, K.; Taniguchi, M.; Kawai, T. *J. Am. Chem. Soc.* **2007**, *129*, 5818.

(32) Monnell, J. D.; Stapleton, J. J.; Dirk, S. M.; Reinert, W. A.; Tour, J. M.; Allara, D. L.; Weiss, P. S. *J. Phys. Chem. B* **2005**, *109*, 20343.

(33) Engelkes, V. B.; Beebe, J. M.; Frisbie, C. D. *J. Am. Chem. Soc.* **2004**, *126*, 14287.

(34) Standard, J. M.; Gregory, B. W.; Clark, B. K. *THEOCHEM* **2007**, *803*, 103.

(35) Mankefors, S.; Grigoriev, A.; Wendin, G. *Nanotechnology* **2003**, *14*, 849.

(36) Hohenberg, P.; Kohn, W. *Phys. Rev.* **1964**, *136*, 864.

(37) Kohn, W.; Sham, L. *Phys. Rev.* **1965**, *140*, 1133.

Chart 1

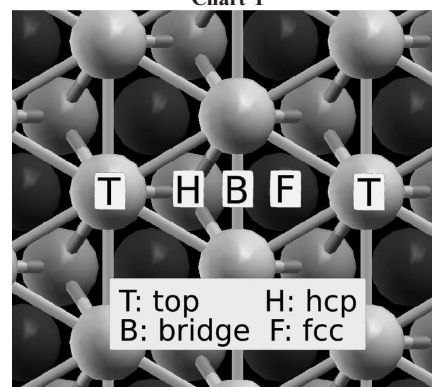


Table 1. Binding Energies on Different High-Symmetry Adsorption Sites for Benzeneselenol, Methylselenol, Benzenethiol, and Methylthiol on the Au(111) Surface

adsorption site	binding energy (kcal/mol)			
	CH ₃ Se–Au	CH ₃ S–Au	C ₆ H ₅ Se–Au	C ₆ H ₅ S–Au
bridge	37.9	36.5	30.6	26.0
fcc	35.5	31.3	29.7	24.7
hcp	33.0	31.0	26.2	24.2
top	30.2	30.5	25.1	23.5

implemented in the Quantum Espresso code,³⁸ which is based on the pseudopotential approximation to represent the ion–electron interactions, and plane waves basis sets to expand the Kohn–Sham orbitals. Ultrasoft type pseudopotentials³⁹ were adopted, in combination with the PBE formalism to compute the exchange–correlation term.⁴⁰ An energy cutoff of 25 and 200 Ry was used to expand the electronic wave functions and the charge density, respectively. The sampling of the Brillouin zone was done with a $2 \times 3 \times 1$ Monkhorst–Pack grid.⁴¹ An energy threshold of 10^{-8} au was used for self-consistency, while for geometry optimizations the applied convergence criteria were of 10^{-4} au on the energy and of 10^{-3} au on the forces per atom. To improve the numerical convergence for the metallic system, a first-order Methfessel–Paxton spreading was implemented.⁴² Both clean and modified surfaces were fully relaxed, with the deepest layer of Au atoms frozen on its bulk position.

III. Results and Discussion

A. Structure and Binding. We explored the binding of methylselenol (SeCH₃) and benzeneselenol (SePh) on the four high-symmetry sites exhibited by the Au(111) surface: top, hcp, bridge, and fcc (see Chart 1).⁴³ To enforce adsorption on the desired site, the binding energy was calculated constraining the x , y coordinates of the link Se atom, while all other degrees of freedom were allowed to relax. The constraint on the x , y coordinates was then removed to get the global energy minimum. An upright configuration was adopted as the starting geometry for the phenyl ring, the molecular plane perpendicular to the surface. Energies for all four adsorption modes are given in Table 1. For both compounds, the most stable interaction involves the bridge site, while the interaction with the top site

(38) Giannozzi, P.; et al. *J. Phys.: Condens. Matter* **2009**, *21*, 395502. <http://www.quantum-espresso.org>.

(39) Vanderbilt, D. *Phys. Rev. B* **1990**, *41*, 7892.

(40) Perdew, J. P.; Burke, K.; Ernzerhof, M. *Phys. Rev. Lett.* **1996**, *77*, 3865.

(41) Monkhorst, H.; Pack, J. *Phys. Rev. B* **1976**, *13*, 5188.

(42) Methfessel, M.; Paxton, T. *Phys. Rev. B* **1989**, *40*, 3616.

(43) The hcp and the fcc sites differ in their relative location with respect to the inner structure: the former is above a Au atom of the second layer, whereas the latter lies over a hollow site.

Table 2. Bond Structure Parameters and Surface to Molecule Charge Transfer Calculated for the Adsorption of Methylselenol, Methylthiol, Benzeneselenol, and Benzenethiol on Au(111)^a

adsorption site	CH ₃ Se–Au			CH ₃ S–Au		
	Au–Se	Au–Se–C	charge transfer	Au–S	Au–S–C	charge transfer
bridge	2.58	107/110	0.11	2.48	110/112	0.23
fcc	2.73	105	0.13	2.50	107	0.29
top	2.49	107	0.24	2.37	109	0.35
hcp	2.71	128	0.16	2.56	128	0.24

adsorption site	C ₆ H ₅ Se–Au			C ₆ H ₅ S–Au		
	Au–Se	Au–Se–C	charge transfer	Au–S	Au–S–C	charge transfer
bridge	2.57	117/120	0.08	2.49	126/128	0.21
fcc	2.71	114	0.17	2.51	114	0.23
top	2.51	119	0.18	2.40	118	0.31
hcp	2.72	118	0.09	2.47	117	0.23

^a Bond lengths in Å, angles in degrees, and charge transfer in *e*.

emerges as the weaker one. The hcp and fcc sites show an intermediate behavior. Even though the top orientation exhibits the shortest bond lengths, the interaction is strengthened by the multiple-fold coordination existent in the other configurations. The values presented for the bridge mode correspond to the full optimization of the adsorbate. Figure 1 displays such relaxed geometries in the most stable binding mode. As far as we are aware, the only discussion about the binding geometry of selenols can be found in a paper by Monnell and collaborators,¹⁸ in which they concluded from STM experiments that the adsorption of alkaneselenolates shows a variability in the binding site involving both bridge and 3-fold hollow sites. In that study, carried out at high coverages for alkyl chains of 10–12 carbons, the authors argued that the structure of the monolayer is controlled by both headgroup–headgroup as well as headgroup–substrate interactions. For the latter kind of interaction, our own calculations predict that the bridge-binding is only slightly favored over the fcc-hollow orientation, with differences in energy of 0.9 kcal/mol for SePh and 2.4 kcal/mol for SeCH₃ (Table 1). According to these results, a competition between the two sites is likely to exist, bringing new theoretical evidence in support of the STM data regarding the adsorption mode of selenolates on gold.

Presently, an open debate subsists in the literature concerning the strength of the Se–Au bond in relation to S–Au. A number of articles, starting from the early work of Samant et al.¹³ to more recent experiments including thermal desorption spectroscopy, XPS, and STM measurements²⁰ concluded that the thiolate–gold interaction is more stable than the selenolate–gold interaction. This is in contrast with results from other researchers based on independent techniques, for example, STM,¹⁴ surface-enhanced Raman spectroscopy,¹⁵ electrochemistry,¹⁹ XPS,^{22,25} among others. As we can see in Table 1, our calculations are in agreement with this second standpoint, suggesting that, for the same chain, selenolates have a slightly stronger interaction with the Au surface than thiolates. In the methyl derivatives, we find a further stabilization on the bridge site of 1.4 kcal/mol and of 2–4 kcal/mol at the 3-fold hollow sites. In the case of the phenyl derivatives, the bond with the gold slab at the bridge site is 4.6 kcal/mol stronger when it is mediated by selenium instead of sulfur, and a

similar trend is found for the other adsorption configurations. We note that the absolute adsorption energies in Table 1 are in very good agreement with data based on thermal desorption spectroscopy for benzeneselenol monolayers on Au(111).²⁰ The reported values of 28.9 and 30.1 kcal/mol attributed respectively to the desorption of diluted phases of SPh and SePh compare well with the calculated energies of 26.0 and 30.6 kcal/mol for the same adsorbates, despite the difference in the molecular configurations.⁴⁴ In any case, binding energy differences between selenols and thiols are not large and account for the divergence in the reported behavior of the interface, eventually controlled by other factors such as interchain forces, rugosity of the surface, coverage, and so on. Overall, these results suggest that, providing the same conditions are given for thiolates and selenolates, a monolayer based on the latter would give stronger adsorbate–surface interactions. Bond lengths are about 0.1 Å longer in selenolates, and there is no significant difference between the alkyl and phenyl species (see Table 2). In spite of this, we can see that the SeCH₃ group presents a linkage 7 kcal/mol stronger than the SPh radical, a trend which is also manifested in the case of thiols.

Valence electronic states of selenium are more diffuse and certainly more extended in space than those of sulfur. Thereafter, the comparable binding energies exhibited by selenols and thiols is somehow an unexpected feature which deserves consideration. The strength of molecular chemisorption can be qualitatively rationalized in terms of different ingredients; among the most important ones are (i) the orientation and availability of the valence orbitals of the adsorbate, (ii) the overlap between such orbitals and the band structure of the surface, (iii) the polarization or covalency of the bond, and (iv) the interatomic distance. All these four are interrelated, and they are but different manifestations of the same quantum–mechanical interaction, yet in practice it could be helpful to appraise each of them separately. Clearly, in terms of the number of valence orbitals and their symmetry, the first ingredient is alike for Se or S. In Figure 2, we investigate the second one: the graph represents the electronic density of states (DOS) projected on the p orbitals of the bound atom (Se or S), confronted with the DOS associated with the d-band. As will be discussed in the following section, these are the electronic states mostly responsible for the bond between the radical and the surface. The valence levels of Se and S appear at similar energies, and therefore, no significant differences are seen in their overlap with the d-states of the slab. The coincidence in binding energies can thus be tracked down to the p levels of Se and S in their alkyl or phenyl derivatives falling very close to each other, probably because of a compensation between exchange–correlation and nuclear attraction effects. The equivalency

(44) Geometry optimizations of SePh and SPh on gold led to upright molecular configurations, with the plane of the benzenes forming an angle close to 80° with respect to the Au surface. On the other hand, data in ref 20 have been assigned via NEXAFS to lying molecules. The reported experimental tilt angles in the denser phases of the SePh and SPh films were 71° and 36°, respectively, and 21° in the diluted phases. These large differences confronting the experimental and the computed tilts can be ascribed to the well-known DFT shortcomings to represent the van der Waals forces operative in between aromatic rings and between these rings and the surface.

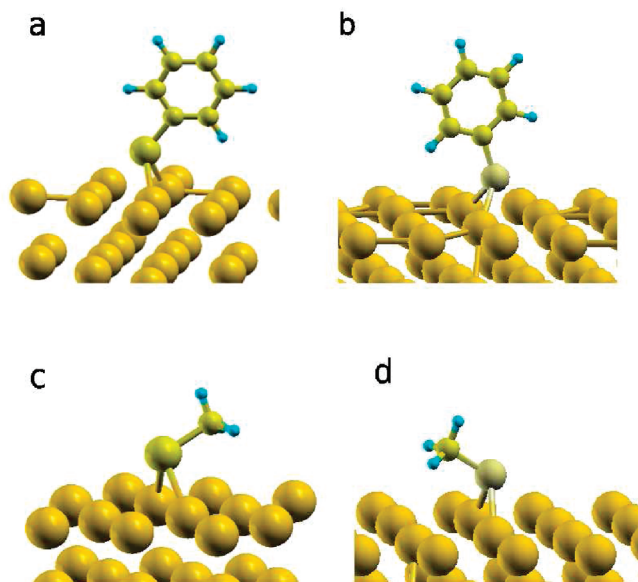


Figure 1. Optimized structures of molecular species on the Au(111) surface: (a) benzeneselenol, (b) benzenethiol, (c) methylselenol, and (d) methylthiol. All optimizations lead to the bridge adsorption mode.

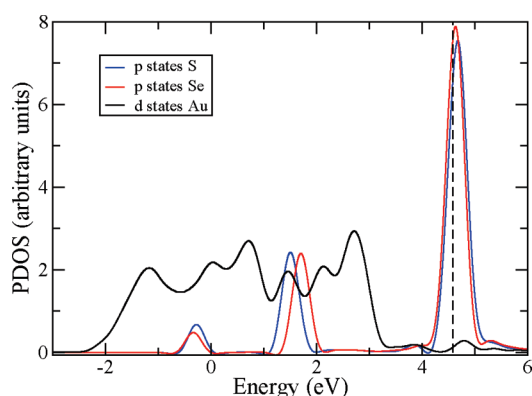


Figure 2. Density of states projected on the d states of an atom of the clean surface, contrasted with the projections on the p orbitals of Se and S in isolated SePh and SCH₃, respectively.

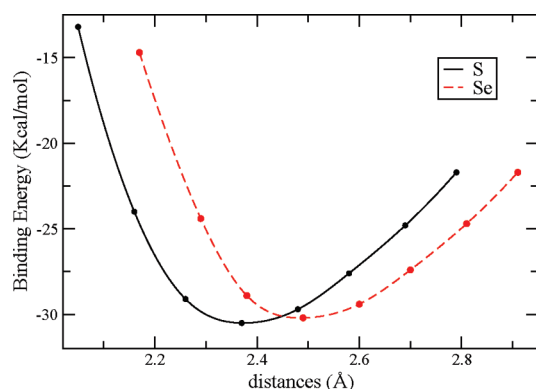


Figure 3. Binding energy of methylselenol and methylthiol to Au(111) for on-top adsorption, as a function of the Se–Au and S–Au distances.

between the strength of these two bonds may be appreciated in Figure 3, which depicts the adsorption energy as a function of the distance from the headgroup to the surface. For simplicity,

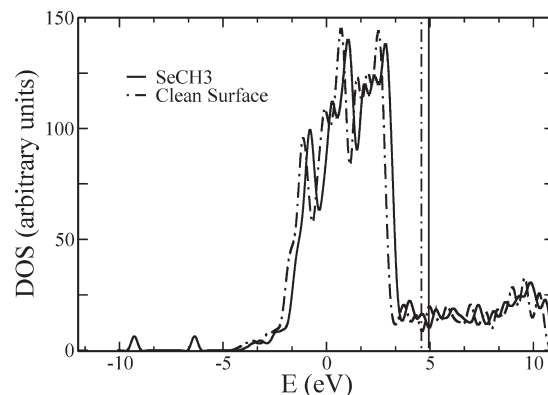


Figure 4. Total density of states for methylselenol adsorbed on gold and for the clean surface. Vertical lines indicate the Fermi level for each case.

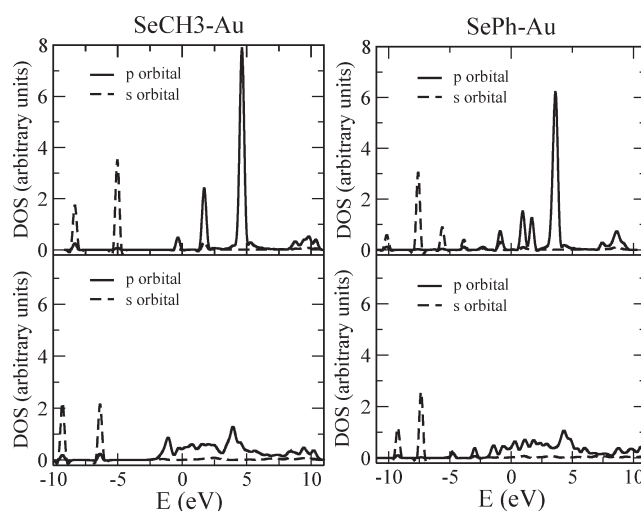


Figure 5. Density of states projected on the s and p orbitals of the Se atom for benzene and methylselenol. Upper panels show the PDOS for the isolated selenols, while lower panels correspond to the molecules adsorbed on the bridge site.

calculations correspond to the top site. Apart from being shifted in the x coordinate, the two curves exhibit no major differences: the identical curvatures around the minima suggest that both the Se–Au and the S–Au bonds could be possibly described with the same force constant. Figure 3 then confirms that the accord in binding energies is not incidental but arises from the very similar nature of both interactions. Charge distributions and the polarization across the bond, on the other hand, are subjects of discussion in the next section.

B. Electronic Structure. Figure 4 shows the total density of states for the Au slab in the absence and in the presence of the chemisorbed methylselenol. It can be seen that the molecule does not affect the DOS pattern to any relevant extent: both curves are shifted with respect to each other consistently with the difference in the number of electrons, exhibiting no gap at the Fermi level, as is proper of metallic systems. The projected density of states (PDOS), which provides information about the involvement of a given atomic orbital in the electronic structure of an extended system, is depicted in Figure 5 for SeCH₃ and SePh. In particular, this figure presents the p and s projections of the Se atom on the total DOS, for both the isolated and the adsorbed radicals. In the isolated cases, a series of sharp peaks can be identified with the discrete lines corresponding to the orbital energies of a finite

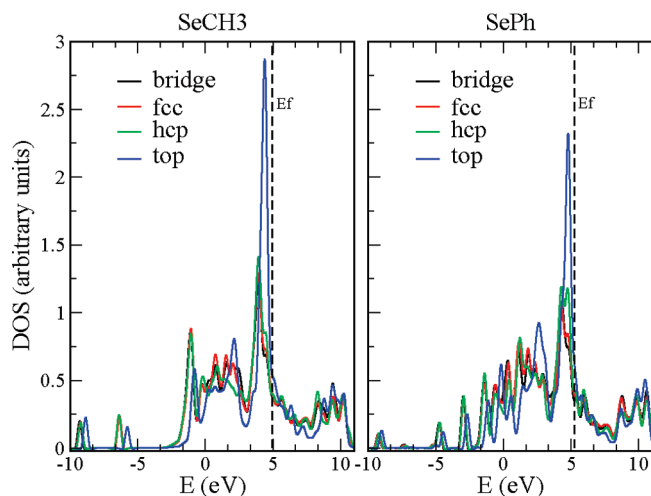


Figure 6. Density of states projected on the p orbitals of the Se atom for benzene and methylselenol, adsorbed on different high-symmetry sites.

system. While the s orbitals are hardly affected upon binding, the p orbitals undergo a significant delocalization across the energy spectrum, indicative of a strong electronic coupling between the molecule and the surface. If the projection is decomposed in its x , y , z orientations (not shown), it is found that the coupling is more pronounced for the p components perpendicular to the surface, where symmetry is more appropriate to hybridize with the d orbitals of the Au atoms. In fact, the PDOS for the p orbitals of Se in the different adsorption sites look quite similar, with the exception of the on-top binding mode, for which the p components parallel to the surface (p_x and p_y) remain highly localized (Figure 6). In other words, the σ bond in Se–Au results from the mixing between the p_{\perp} orbitals of the link atom and the d states of the metal, with little or no participation of the s states. This hybridization involving such a broad delocalization has been already reported by us for the adsorption of thiols, and it is in sharp contrast with what is observed for other kinds of binding as in C–Au.⁶ To assess quantitatively the extent of delocalization of a given orbital q , we define a delocalization index $I(q) = \max[\int D_i(\epsilon) D_f(\epsilon - \epsilon_0) d\epsilon]$, with D_i and D_f being the normalized partial density of states associated with q before and after binding.⁴⁵ This index may vary from 1 when there is no delocalization ($D_i(\epsilon) = D_f(\epsilon)$) to nearly 0 when the final PDOS departs substantially from its initial distribution. Evaluation of $I(q)$ for the p orbitals of carbon in AuCH₂CH₃, of selenium in AuSeCH₃, and of sulfur in AuSCH₃ gives 0.67, 0.60, and 0.57, respectively, indicating that the degree of delocalization in Se–Au falls in between C–Au and S–Au, but closer to the latter. Similar numbers are found for the aromatic adsorbates.

Table 3 presents the work functions Φ corresponding to the Au(111) surface with all four adsorbates at their minimum energy configurations. The calculated Φ for the clean surface is 5.29 eV, in excellent accord with photoemission experiments.⁴⁶ Aliphatic thiols and selenols produce a decrease of less than 0.1 eV in Φ with respect to clean Au(111), while for the aromatic adsorbates the decay is twice as much: the magnitude of the effect depends on the

Table 3. Work Functions (Φ) and Charge Transfer (CT) from the Headgroup to the Adjacent Carbon, Calculated for Methylselenol, Methylthiol, Benzeneselenol, and Benzenethiol on Au(111) at the Minimum Energy Configurations

	Au–SeCH ₃	Au–SCH ₃	Au–SePh	Au–SPh
Φ (eV)	5.20	5.21	5.12	5.12
CT (e)	0.57	0.54	0.59	0.60

organic function rather than on the headgroup. We note the decrease in the work function is significantly smaller than that reported in previous DFT studies of methylthiol SAMs on gold,^{47,48} essentially because those simulations considered a densely packed phase (1 molecule per $\sqrt{3} \times \sqrt{3}$ R30° surface unit cell), whereas our calculations represent the dilute regime which avoids adsorbate–adsorbate interactions, with a coverage of 1.15 molecules/nm².

The integration of the total DOS up to the Fermi level provides the number of electrons in the system. On the other hand, if the integration is restricted to the density of states projected onto the orbitals of certain atoms, it is possible to obtain the number of electrons associated with those atoms only. To get an estimate of the metal to molecule charge transfer, we have integrated the PDOS involving the atomic orbitals of the Au centers and subtracted it from the number of electrons corresponding to the isolated slab. The results, collected in Table 2, are always greater than zero, implying a charge transfer from the surface to the adsorbate, so that the bond can be represented as Se^{δ−}–Au^{δ+}. The same polarization across the molecule–metal axis has been proposed for S–Au and C–Au.^{6,49}

The extent of charge transfer is smaller in selenols than in thiols for the same binding mode, and it can be seen that it is enhanced in the less stable configurations. Interestingly, in agreement with our results, the ionic character of the bond has been recently predicted from XPS to be higher in S–Au than in Se–Au.³¹ As discussed elsewhere,⁶ in an ideal molecular contact, as in a perfect conductor, the potential must be homogeneous along the junction, in opposition to an ionic system, for which the charge accumulates or depletes at either side of the bond. That is to say, the more polarized the bond is at zero bias, the larger the resistance that can be expected to electron transport. Therefore, the results in Table 2 seem to indicate that the Se–Au junction would offer a better conductance than S–Au. This is in line with previous calculations of quantum transport^{26–28} and with data from different experimental techniques such as STM^{29,30} and UPS³¹ but in contrast with conclusions derived from some more recent STM measurements.³² As a matter of fact, scanning tunneling microscopies have led researchers to contradictory interpretations. On the one hand, Bourgoin and co-workers found that apparent heights for terthiophenes anchored through sulfur were statistically more significant than those for terthiophenes attached via selenium, suggesting that the latter provides a better metal–molecule electronic coupling.^{29,30} Tunneling currents were collected from terthiophene molecules and aggregates inserted in a matrix of dodecanethiol. On the other hand, based also on STM, Monnell et al. claimed the opposite behavior.³² The observed STM current at a monolayer is the outcome of several factors, including surface geometry, local packing, lateral interactions, and the resistance in at least two contacts. In ref 32, these effects were individualized throughout a careful treatment, to extract the particular

(45) The choice of an index to measure the delocalization degree is not unique: the formula proposed here is just one out of many possible criteria. $I(q)$ seeks the maximum overlap between the initial and final PDOS for all possible shifts in energy ϵ_0 . Under this definition, a perturbation that only displaces the center of the PDOS to lower or higher energies, without really affecting its shape, would return $I(q) = 1$, detecting no delocalization.

(46) Hansson, G. V.; Flodström, S. A. *Phys. Rev. B* **1978**, *18*, 1572.

(47) Rusu, P. C.; Brocks, G. *J. Phys. Chem. B* **2006**, *110*, 22628.

(48) Nagoya, A.; Morikawa, Y. *J. Phys.: Condens. Matter* **2007**, *19*, 365245.

(49) Gronbeck, H.; Curioni, A.; Andreoni, W. *J. Am. Chem. Soc.* **2000**, *122*, 3839.

contributions of the Se–Au and S–Au contacts to the overall conductance. Mixed SAMs of alkanethiolates and alkaneselenolates were prepared and sensed on the same platform, to probe side by side relative conductances. The authors estimated that alkanethiolates were more conductive than equivalent alkaneselenolates by a factor of 2.5. This contradiction between experiments is certainly intriguing, even more so when both were based on state of the art techniques in controlled conditions and provided conclusive data.

An obvious argument to reconcile the above issue is that the relative conductances across the S–Au and Se–Au junctions are inverted in terthiophenes with respect to alkanes. There is no evident reason why this should happen, and in principle this explanation seems unlikely, but it might be worth of further investigation. It is suggestive that UPS and XPS experiments, which determined that Se involves lower charge injection barriers from gold,³¹ were performed on the phenyl derivatives. Furthermore, quantum transport calculations indicating higher conductances at Se–Au dealt with conjugated molecules.^{26–28} In this line of thought, it could be conjectured that a conjugated backbone causes an inversion in the relative transport rates between S–Au and Se–Au. Discrepancies might then be explained in terms of differences in intramolecular conductance originating in the C–Se and C–S bonds, meaning that the availability of π -conjugated electrons allow for a more efficient transport across C–Se, and vice versa. If this were demonstrated, the controversy between experiments would be settled. The results for electron transfer calculations from the slab, now including the head-group, to the adjacent carbon in SePh, SeCH₃, SPh, and SCH₃ are summarized in Table 3. It can be seen that the polarization of the bond is larger in SeCH₃ than in SCH₃ but smaller in SePh than in SPh. Unfortunately, even if these data seem to be consistent with the hypothesis above, the observed trends are too moderate to be conclusive and cannot be taken as definite evidence to support the presumed effect of conjugation. We are still far from a final answer, and inconsistencies between experiments continue to be puzzling, but we hope this discus-

sion has highlighted the need for new experiments and simulations able to reconcile the existing data.

IV. Conclusions

The present calculations suggest that self-assembled monolayers of selenols would exhibit marginally larger stabilities than SAMS based on thiols. Energy differences between the two kinds of bonds are small enough as to be shadowed by other effects, for example, interactions between organic chains or defects on the metal substrate. In any case, these minor differences explain why there has not been universal agreement as for the relative stability of these two types of SAMs. The bridge binding mode ascribed to thiols on gold is found also for selenols as the most stable configuration. On the other hand, the examination of the projected density of states of the S and Se systems reveals a very similar pattern, quite different from the one found for carbon.⁶ However, the charge transfer across the Se–Au bond is less pronounced than that in S–Au, which is indicative of a less ionic (or more metallic) bond, and therefore, it can be speculated that selenium monolayers will offer better conduction properties. This result is consistent with experiments and previous quantum calculations performed on π -conjugated molecules on Au, but at the same time it is in apparent contradiction with experimental findings on aliphatic SAMs.³² An obvious path to explain this disagreement would be to assume that conjugation alters the relative efficiency of metal to molecule electron transport. Nevertheless, existing data are far from being conclusive in this respect, and further research from both the experimental and the theoretical areas would be required to give a definite answer to the question regarding the relative conductance of S–Au and Se–Au contacts.

Acknowledgment. We thank the reviewers for pointing out very pertinent unnoticed work, for helpful remarks, and for constructive criticism. This work was supported by funding granted to D.A.S. by CONICET (PIP5520) and ANPCYT (PICT06-33581 and PICT 2007-02111). E.dL. acknowledges CONICET for a doctoral fellowship.